

# Spontaneous quantum Hall effect in an atomic spinor Bose-Fermi mixture

Zhi-Fang Xu,<sup>1</sup> Xiaopeng Li,<sup>2</sup> Peter Zoller,<sup>3,4</sup> and W. Vincent Liu<sup>1</sup>

<sup>1</sup>*Department of Physics and Astronomy, University of Pittsburgh, Pittsburgh, Pennsylvania 15260, USA*

<sup>2</sup>*Condensed Matter Theory Center and Joint Quantum Institute,*

*Department of Physics, University of Maryland, College Park, MD 20742-4111, USA*

<sup>3</sup>*Institute for Quantum Optics and Quantum Information of the Austrian Academy of Sciences, A-6020 Innsbruck, Austria*

<sup>4</sup>*Institute for Theoretical Physics, University of Innsbruck, A-6020 Innsbruck, Austria*

(Dated: July 15, 2014)

We study a mixture of spin-1 bosonic and spin-1/2 fermionic cold atoms, e.g., <sup>87</sup>Rb and <sup>6</sup>Li, confined in a triangular optical lattice. With fermions at 3/4 filling, Fermi surface nesting leads to spontaneous formation of various spin textures of bosons in the ground state, such as collinear, coplanar and even non-coplanar spin orders. The phase diagram is mapped out with varying boson tunneling and Bose-Fermi interactions. Most significantly, in one non-coplanar state the mixture is found to exhibit a spontaneous quantum Hall effect in fermions and crystalline superfluidity in bosons, both driven by interaction.

PACS numbers: 03.75.Mn, 67.85.Pq, 75.10.-b, 11.30.Qc

*Introduction.* Searching for topological states of quantum matter, such as quantum Hall states and topological insulators, is one of the most important directions in ultracold atoms. To achieve such novel states in a charge neutral system, external manipulations to synthesize effective gauge fields [1] have been carried out, for example, by rotating the system [2], using Raman laser field coupling schemes [3–10], or shaking the lattice [11–14]. At present the realization of topological states has remained an experimental challenge. An alternative route is to have fermions move in a spontaneous spin texture background [15–20]. In cold atomic systems, pioneer studies suggest that spatially varying magnetic fields [21, 22] or magnetic dipolar interactions [23–30] could lead to interesting spin modulations including textures in purely bosonic systems. The possible topological states of fermions loaded into such synthesized topological configurations have yet to be studied for cold atoms. Furthermore, it is worth finding out whether a short-range interaction, dominant over other forms of interaction in the extensively studied alkali metal cold gases, can give rise to spontaneously generated spin textures in the absence of applied magnetic fields.

In this Letter, we first show that topologically nontrivial spin textures can be naturally stabilized in an atomic mixture of spin-1 bosons and spin-1/2 fermions, e.g., <sup>87</sup>Rb and <sup>6</sup>Li, loaded into a two-dimensional triangular optical lattice. The underlying reason is that fermions mediate an effective long-range interaction analogous to the Ruderman-Kittel-Kasuya-Yosida (RKKY) interaction for spinor bosons [31], which leads to spin modulations in the ground state. Spin textures then provide effective gauge fields as an important feedback to fermions. This effect as an interplay in the spinor Bose-Fermi mixture is amplified when the Fermi surface is nested at 3/4 filling [18]. We

study the ground state at this filling via a self-consistent mean-field approach and find various topologically distinct spin textures such as collinear, coplanar and even non-coplanar ones. Remarkably, in one non-coplanar state, fermions and bosons spontaneously form a quantum Hall state and a chiral superfluid state, respectively.

This work thus points to a mechanism for spin textures and topological states to emerge in an atomic system in the absence of external fields like an artificial gauge field, rotation, or their equivalent. For the potential experimental observation of the quantum Hall related phases, our model has a crucial advantage, as the minimal condition to realize it appears well satisfied by two well-established experimental capabilities: mixing different atomic species and creating triangular optical lattices.

*Spinor Bose-Fermi mixture.* Consider a mixture of spin-1 bosonic and spin-1/2 fermionic cold atoms. There will be the usual density and spin interactions between two particles in the same species [32, 33]. The crucial new ingredient is the interaction between the species of bosons and fermions, which is described by the contact pseudo-potential

$$V_{bf}(\mathbf{r}_1 - \mathbf{r}_2) = \left( g_{\frac{1}{2}} \hat{\mathcal{P}}_{\frac{1}{2}} + g_{\frac{3}{2}} \hat{\mathcal{P}}_{\frac{3}{2}} \right) \delta(\mathbf{r}_1 - \mathbf{r}_2), \quad (1)$$

where  $g_{F_{\text{tot}}} = 2\pi\hbar^2 a_{F_{\text{tot}}}/m_{bf}$  is the s-wave scattering length in the channel of total spin  $F_{\text{tot}}$ ,  $\hat{\mathcal{P}}_{F_{\text{tot}}}$  is the corresponding projection operator, and  $m_{bf}$  is the reduced mass. Based on the identity  $2\hat{\mathbf{S}} \cdot \hat{\mathbf{F}} = \hat{\mathcal{P}}_{3/2} - 2\hat{\mathcal{P}}_{1/2}$  [32], where  $\hat{\mathbf{S}}$  and  $\hat{\mathbf{F}}$  are the one-particle vector spin for spin-1/2 and spin-1 atoms, respectively. The Bose-Fermi contact interaction can be rewritten as

$$V_{bf}(\mathbf{r}_1 - \mathbf{r}_2) = \left( g_d \hat{I}_S \otimes \hat{I}_F + g_s \hat{\mathbf{S}} \cdot \hat{\mathbf{F}} \right) \delta(\mathbf{r}_1 - \mathbf{r}_2), \quad (2)$$

where  $g_d = (g_{1/2} + 2g_{3/2})/3$  and  $g_s = (2g_{3/2} - 2g_{1/2})/3$  are the density-density interaction and spin-exchange interaction strengths, respectively. Here,  $\hat{I}_S$  ( $\hat{I}_F$ ) is the identity operator for the fermion (boson).

With the spinor Bose-Fermi mixture loaded into a triangular optical lattice, the system is approximately described by a tight-binding model Hamiltonian

$$\begin{aligned}\hat{H} &= \hat{H}_b + \hat{H}_f + \hat{H}_{bf}, \\ \hat{H}_f &= -t_f \sum_{\langle i,j \rangle, \sigma} \hat{c}_{i,\sigma}^\dagger \hat{c}_{j,\sigma} + U_f \sum_i \hat{n}_{f,i,\uparrow} \hat{n}_{f,i,\downarrow}, \\ \hat{H}_b &= -t_b \sum_{\langle i,j \rangle, \alpha} \hat{b}_{i,\alpha}^\dagger \hat{b}_{j,\alpha} + \frac{U_b}{2} \sum_i \hat{n}_{b,i} (\hat{n}_{b,i} - 1) \\ &\quad + \frac{J_b}{2} \sum_i (\hat{\mathbf{F}}_i^2 - 2\hat{n}_{b,i}), \\ \hat{H}_{bf} &= U_{bf} \sum_i \hat{n}_{f,i} \hat{n}_{b,i} + J_{bf} \sum_i \hat{\mathbf{S}}_i \cdot \hat{\mathbf{F}}_i,\end{aligned}\quad (3)$$

where  $\langle i, j \rangle$  denotes the summation over nearest-neighbor sites and  $\sigma = \uparrow, \downarrow$  and  $\alpha = +1, 0, -1$  denote spin states of fermionic and bosonic atoms, respectively.  $\hat{c}_{i\sigma}$  ( $\hat{a}_{i\alpha}$ ) is the annihilation operator for fermions (bosons) with spin  $\sigma$  ( $\alpha$ ).  $\hat{n}_{f,i} = \sum_{\sigma} \hat{n}_{f,i,\sigma} = \sum_{\sigma} \hat{c}_{i,\sigma}^\dagger \hat{c}_{i,\sigma}$  ( $\hat{n}_{b,i} = \sum_{\alpha} \hat{n}_{b,i,\alpha} = \sum_{\alpha} \hat{b}_{i,\alpha}^\dagger \hat{b}_{i,\alpha}$ ) is the number of fermions (bosons) at site  $i$ . The spin operator  $\hat{\mathbf{S}}_i$  ( $\hat{\mathbf{F}}_i$ ) has three components  $\hat{S}_{i\nu} = \sum_{\sigma\sigma'} \hat{c}_{i,\sigma}^\dagger (S_\nu)_{\sigma\sigma'} \hat{c}_{i,\sigma'}$  ( $\hat{F}_{i\nu} = \sum_{\alpha\alpha'} \hat{b}_{i,\alpha}^\dagger (F_\nu)_{\alpha\alpha'} \hat{b}_{i,\alpha'}$ ) with  $\nu = x, y, z$ , where  $S_\nu$  ( $F_\nu$ ) is the  $\nu$  component of the spin-1/2 (spin-1) operator.  $U_f$ ,  $U_b$ , and  $U_{bf}$  represent on-site density-density interaction strengths, and  $J_b$  and  $J_{bf}$  are the spin-exchange interaction energies. The exchange interaction  $J_b < 0$  favors a state with the spins of bosons locally fully polarized [34, 35]. Such a ferromagnetic interaction is considered in this work. Considering a mixture of  $^{87}\text{Rb}$  and  $^6\text{Li}$  atoms, the s-wave scattering length for fermions,  $^6\text{Li}$ , vanishes due to an accidental cancellation at low magnetic field [36, 37], and  $U_f$  is thus set to be 0 in our theory.

*Magnetic ordering of bosonic superfluids.* Here, our theory assumes bosons form a ferromagnetic minicondensate on each lattice site. Such a treatment is well justified when considering the system to be a stack of triangular lattice layers, with a relatively stronger tunneling for bosons than for fermions between nearest layers. In the ground state, the system is uniform among different layers. Quantum fluctuations of bosonic spins are expected to be suppressed in such a quasi-two-dimensional layer, which permits a valid mean field treatment of the system.

For spin-1/2 fermions, at 3/4 filling (meaning  $(1/2N_L) \sum_i \langle \hat{n}_{f,i} \rangle = 3/4$  with  $N_L$  is the number of sites), the corresponding Fermi surface as shown in Fig. 1(b) is nested, with three nesting vectors  $\mathbf{Q}_1 = (2\pi/a, 0)$ ,  $\mathbf{Q}_2 = (\pi/a, \sqrt{3}\pi/a)$  and  $\mathbf{Q}_3 = (\pi/a, -\sqrt{3}\pi/a)$ , where  $a$  is the lattice constant. Combined with Bose-Fermi

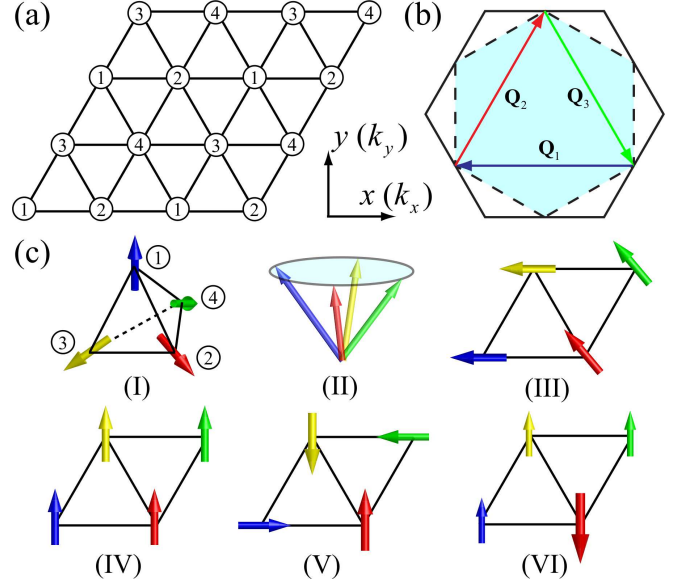


FIG. 1: (a) Schematic picture of a triangular optical lattice and the four-sublattice magnetic ordering. (b) The Brillouin zone of the triangular lattice (solid hexagon) and the Fermi surface (dashed hexagon) for the 3/4 filling. Three nesting wave vectors are  $\mathbf{Q}_1 = (2\pi/a, 0)$ ,  $\mathbf{Q}_2 = (\pi/a, \sqrt{3}\pi/a)$  and  $\mathbf{Q}_3 = (\pi/a, -\sqrt{3}\pi/a)$  where  $a$  is the lattice constant. (c) The spin configuration of six different magnetic orderings of the spin-1 Bose-Einstein condensate, where the arrows denote the direction of four spin vectors  $\langle \hat{\mathbf{F}}_i \rangle$  ( $i = 1, 2, 3, 4$ ): (I) all-out structure chiral spin order; (II) “umbrella” structure spin order, where the end points of four spin vectors locate on the same plane; (III) stripe-cant spin order; (IV) ferromagnetic order; (V) coexistence of DW and  $90^\circ$  coplanar spin order; and (VI) coexistence of DW and collinear spin order.

density and spin-exchange interactions, the perfect Fermi surface nesting gives rise to ordering instabilities towards formation of commensurate density waves (DWs) and spin density waves (SDWs) whose unit cells would involve four sublattice sites, shown in Fig. 1 [18, 19, 38].

From the dominant instabilities, we assume in numerics that spin-1 bosons form a magnetic ordering where the density  $n_{b,i} = \langle \hat{n}_{b,i} \rangle$  and the spin vector  $\langle \hat{\mathbf{F}}_i \rangle$  are periodic under translations of the enlarged unit cell (Fig. 1). Within the superfluid phase, we take mean-field approximations for bosons, where the bosonic annihilation operator  $\hat{b}_{i,\alpha}$  is replaced by its mean value  $\phi_{i,\alpha}$ . Both the intraspecies ferromagnetic interaction of bosons and the interspecies spin-exchange interaction favor a state of the condensate with spins fully polarized locally. The corresponding condensate wavefunction is  $\phi_i = \sqrt{n_{b,i}} e^{i\xi_i} \zeta_i$ , where

$$\zeta_i = \left( e^{-i\varphi_i} \cos^2 \frac{\theta_i}{2}, \frac{\sin \theta_i}{\sqrt{2}}, e^{i\varphi_i} \sin^2 \frac{\theta_i}{2} \right)^T, \quad (4)$$

which yields the spin moment  $\langle \hat{\mathbf{F}}_i \rangle = \sqrt{n_{b,i}} (\sin \theta_i \cos \varphi_i, \sin \theta_i \sin \varphi_i, \cos \theta_i)$ . In our calculation,

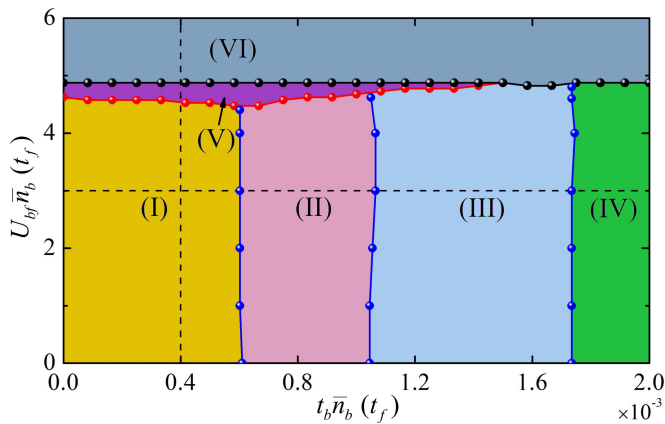


FIG. 2: Zero temperature phase diagram of spinor Bose-Fermi mixtures in a triangular lattice at 3/4 filling for fermions,  $(U_b + J_b)\bar{n}_b^2 = 14.4t_f$ , and  $J_{bf}\bar{n}_b = 0.8t_f$  as functions of  $t_b\bar{n}_b$  and  $U_{bf}\bar{n}_b$ , where  $U_b > 0 > J_b$  and  $\bar{n}_b$  is the averaged number of bosons per site. Physical quantities along two dashed lines are shown in Fig. 3.

we allow for a finite-momentum condensation by introducing a parametrization of the phase,  $\xi_i = \mathbf{q} \cdot \mathbf{r}_i + \tilde{\xi}_i$ , where nonzero  $\mathbf{q}$  describes the finite momentum and  $\tilde{\xi}_i$  is periodic across different enlarged unit cells.

With spin configuration of bosons determined by a fixed condensate wavefunction  $\phi_i$ , the dynamics of fermions is governed by an effective Hamiltonian:

$$\hat{H}_f^{\text{eff}} = -t_f \sum_{\langle i,j \rangle, \sigma} \hat{c}_{i,\sigma}^\dagger \hat{c}_{j,\sigma} + \sum_i [U_{bf} \langle \hat{n}_{b,i} \rangle \hat{n}_{f,i} + J_{bf} \langle \hat{\mathbf{F}}_i \rangle \cdot \hat{\mathbf{S}}_i].$$

The total energy cost is given by  $E[\phi_i] = E_b[\phi_i] + E_f[\phi_i]$ , where  $E_b = -t_b \sum_{\langle i,j \rangle, \alpha} \phi_{i,\alpha}^* \phi_{j,\alpha} + \sum_i [U_b n_{b,i} (n_{b,i} - 1) + J_b (n_{b,i}^2 - 2n_{b,i})]/2$  describes the energy of the condensate and  $E_f$  is the many-body ground state energy of fermions at 3/4 filling with respect to  $H_f^{\text{eff}}$  (in our numerics to calculate  $E_f$ , we discretize the first Brillouin zone into  $72 \times 72$  points). The variational energy functional  $E[\phi_i]$  is then minimized by the simulated annealing method to obtain the ground state.

Figure 2 summarizes the ground-state phase diagram for a fixed  $J_{bf}\bar{n}_b$  as functions of  $t_b\bar{n}_b$  and  $U_{bf}\bar{n}_b$ , where  $\bar{n}_b$  is the averaged number of bosons per site. In the limit of  $U_{bf} = 0$  and  $t_b = 0$ , the system is described by a classical Kondo lattice model [18, 19], where chiral magnetic orders in the ground state are known to occur even with an infinitesimal Kondo coupling  $J_{bf}\bar{n}_b$  due to Fermi surface nesting. Away from this limit, nonzero boson tunneling and Bose-Fermi density interaction change the ground-state magnetic ordering significantly. The former favors a uniform condensate wavefunction to lower the kinetic energy and will thus suppress spin textures. The latter could induce spatially non-uniform density distributions of bosons. Indeed as boson tunneling is increased, our numerics finds a sequence of states with

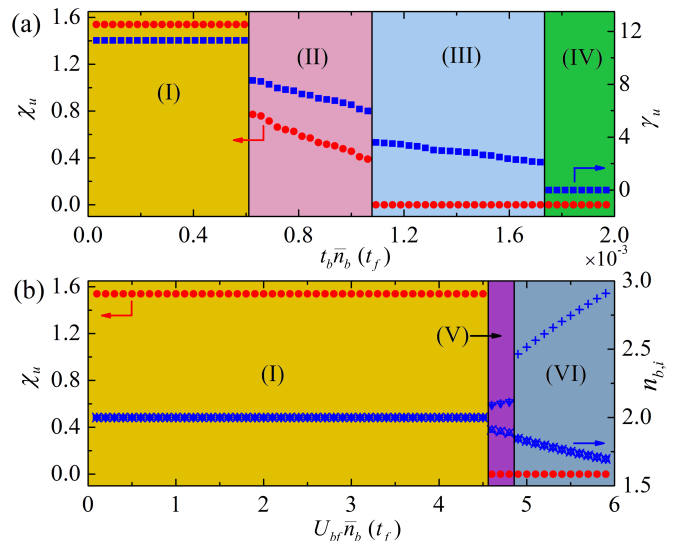


FIG. 3: (a) Scalar spin chirality  $\chi_u \equiv |\chi_{123}| + |\chi_{243}|$  (red filled circles) and  $\gamma_u$  (blue filled squares) defined in a unit cell as a function of  $t_b\bar{n}_b$  at  $U_{bf}\bar{n}_b = 3t_f$ . (b) Local scalar spin chirality  $\chi_u$  (red filled circles) and the number of bosons  $n_{b,i}$  (blue symbols ‘ $\Delta$ ’, ‘+’, ‘ $\times$ ’, ‘ $\nabla$ ’) at site  $i$  ( $i = 1, 2, 3, 4$ ) as a function of  $U_{bf}\bar{n}_b$  at  $t_b\bar{n}_b = 0.4 \times 10^{-3} t_f$ .

decreasing spin twists which are quantified by  $\chi_u$  and  $\gamma_u$  defined below. The corresponding schematic spin configurations are illustrated in Fig. 1(c). As the Bose-Fermi density interaction is increased, we find that two states denoted by phases (V) and (VI) are accompanied by DWs. Here, we want to mention that switching the sign of  $J_{bf}$  only changes the spins of fermions from being anti-aligned to aligned with bosons, without changing the structure of magnetic orderings or the phase boundaries.

(1) **Non-coplanar magnetic ordering.** Numerically, we found two non-coplanar magnetic ordered phases denoted by (I) and (II). To characterize them, we calculate the local spin chirality of bosons on three different lattice sites  $i, j$ , and  $k$  defined as

$$\chi_{ijk} = \frac{\langle \hat{\mathbf{F}}_i \rangle \cdot \langle \hat{\mathbf{F}}_j \rangle \times \langle \hat{\mathbf{F}}_k \rangle}{|\langle \hat{\mathbf{F}}_i \rangle| |\langle \hat{\mathbf{F}}_j \rangle| |\langle \hat{\mathbf{F}}_k \rangle|}. \quad (5)$$

Phase (I) shows the same triple- $\mathbf{Q}$  chiral magnetic ordering found in the Kondo lattice model [18, 19]. The boson number density is uniform with  $n_{b,i} = \bar{n}_b$  and its spin vector takes the form

$$\langle \hat{\mathbf{F}}_i \rangle = (\eta_1 \cos(\mathbf{Q}_1 \cdot \mathbf{r}_i), \eta_2 \cos(\mathbf{Q}_2 \cdot \mathbf{r}_i), \eta_3 \cos(\mathbf{Q}_3 \cdot \mathbf{r}_i)), \quad (6)$$

where  $|\eta_1| = |\eta_2| = |\eta_3| = \bar{n}_b/\sqrt{3}$ . The spin chirality is also uniform with  $\chi_{123} = \chi_{243} = \pm 4/(3\sqrt{3})$  which means that fermions experience an effective uniform magnetic flux. Via coupling to spin textures, fermions are gapped and spontaneously form a quantum Hall insulator [18].

Phase (II) shows a uniform boson density distribution and a non-coplanar magnetic ordering, where four spin

vectors  $\langle \hat{\mathbf{F}}_i \rangle$  form an umbrella structure as illustrated in Fig. 1(c). The end point of four spin vectors locate on the same plane  $\mathcal{O}$  (shaded disk) and form a rectangle, which means  $\mathcal{O} \perp \sum_{i=1}^4 \langle \hat{\mathbf{F}}_i \rangle$ . The local spin chirality is staggered with a zero summation on the whole lattice and its absolute value is uniform. Numerically we use  $\chi_u \equiv |\chi_{123}| + |\chi_{243}|$  to distinguish non-coplanar phases from others.

(2) **Coplanar magnetic ordering.** When bosons form a spontaneous coplanar magnetic ordering, the scalar spin chirality  $\chi_u$  is zero. We thus define another quantity

$$\gamma_{ij} = \frac{\langle \hat{\mathbf{F}}_i \rangle \times \langle \hat{\mathbf{F}}_j \rangle}{|\langle \hat{\mathbf{F}}_i \rangle| |\langle \hat{\mathbf{F}}_j \rangle|}, \quad (7)$$

and use  $\gamma_u = \sum_{i \neq j} |\gamma_{ij}|$  with  $i, j = 1, 2, 3, 4$  to distinguish coplanar and collinear magnetic orderings. Numerically, we find two coplanar phases denoted by (III) and (V).

Within phase (III), bosons are uniformly distributed in every site and four spin vectors form a stripe-cant structure as shown in Fig. 1(c), which are characterized by  $\chi_u = 0$ ,  $\gamma_u \neq 0$ , and  $n_{b,i} = \bar{n}_b$ .

Phase (V) shows a  $90^\circ$  coplanar magnetic ordering accompanied by a DW, where a pair of antiparallel spin vectors have a larger magnitude than another pair of antiparallel spin vectors. From Fig. 3(b), we can infer that the number of bosons  $n_{b,i}$  in four sublattices separate into two different values when falling in the phase (V). As shown in the phase diagram of Fig. 2, this phase appears in a narrow region of the parameter space.

(3) **Collinear magnetic ordering.** The remaining two phases (IV) and (VI) show collinear magnetic orderings on bosons, characterized by  $\chi_u = 0$  and  $\gamma_u = 0$ . More specifically, phase (IV) demonstrates a ferromagnetic spin ordering, where all spins of bosons are polarized along the same direction. Meanwhile, each site has the same number of bosons. When the Bose-Fermi density interaction is strong enough, we obtain phase (VI), in which the collinear spin ordering is accompanied by a DW. The existence of DW can be seen from Fig. 3(b), where the number of bosons on four sublattices have two different values. Full numerical results show that in a four-sublattice unit cell three smaller spin vectors with a same magnitude are polarized along opposite direction of the fourth spin vector with a larger magnitude. The magnetic ordering of phase (VI) is similar to the SDW of electronic systems driven by thermal fluctuations, which was discussed in Ref. [39].

*Chiral bosonic superfluid.* Due to the Bose-Fermi interactions, Fermi surface nesting of fermions not only induces spontaneous spin textures of bosons, but also changes the bosonic superfluidity. The reason is that the spin-gauge symmetry of the ferromagnetic spin-1 BEC implies that spatial spin configurations can generate mass circulations [32, 33], which is manifested in the spatially

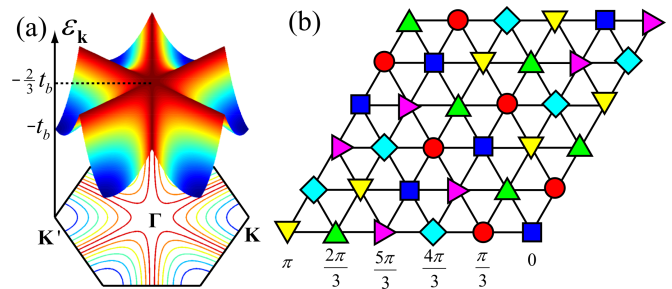


FIG. 4: (a) The lowest energy band of the Hamiltonian (8) with eigen-energy denoted by  $\varepsilon_{\mathbf{k}}$ . (b) Spatial variation of  $\xi_i$  for the phase (I) with  $\mathbf{q} = \mathbf{K}$ , where six symbols are used to denote different values of  $\xi_i$ .

dependent  $\xi_i$ . We find that bosons condense at zero momentum with  $\mathbf{q} = 0$  for phases: (II), (III), (IV), (V), and (VI). The only exception is found in the phase (I), where bosons are condensed at a finite momentum with  $\mathbf{q} \neq 0$ . To understand this feature more clearly, we consider an effective single-particle Hamiltonian

$$\hat{H}_b^{\text{SP}} = - \sum_{\langle i,j \rangle} \tilde{t}_{b,ij} \hat{d}_i^\dagger \hat{d}_j, \quad (8)$$

for spin-1 bosons whose spin directions are fixed as that given by Eq. (6). Here,  $\hat{d}_i^\dagger$  creates a spin-1 boson at site  $i$  with the spin state  $\zeta_i$  and  $\tilde{t}_{b,ij} = t_b \zeta_i^\dagger \zeta_j$  describes the tunneling of bosons in such a spin state. For instance, we choose  $\eta_1 = \eta_2 = \eta_3 = \bar{n}_b / \sqrt{3}$ , resulting in  $\{\varphi_1 = \pi/4, \theta_1 = \arccos(1/\sqrt{3})\}$ ,  $\{\varphi_2 = -\pi/4, \theta_2 = \pi - \theta_1\}$ ,  $\{\varphi_3 = 3\pi/4, \theta_3 = \pi - \theta_1\}$ , and  $\{\varphi_4 = -3\pi/4, \theta_4 = \theta_1\}$ . Diagonalizing the Hamiltonian (8) we find that the lowest energy band shown in Fig. 4(a) has band minima at  $\mathbf{K} = (2\pi/3a, 0)$  and  $\mathbf{K}' = (-2\pi/3a, 0)$ . The corresponding eigenstates have equal populations on each site. These two features are underlying reasons for finite-momentum condensation and uniform density distribution of bosons in the phase (I) as found in numerics. Take  $\mathbf{q} = \mathbf{K}$  as an example, the spatial variation of  $\xi_i$  is illustrated in Fig. 4(b). As  $\mathbf{q}$  is nonzero, bosons condense at a nonzero momentum, thus time-reversal and parity symmetries are broken.

*Experimental realization and detection.* The model of Eq. (3) can be realized by loading a mixture of spin-1/2  $^6\text{Li}$  and spin-1  $^{87}\text{Rb}$  atoms [40] in the same spin-independent triangular optical lattice. For instance, we choose laser fields at wavelength  $\lambda = 1064$  nm. The single photon recoil energy  $E_r$  and polarizability  $\alpha(\lambda)$  for  $^{87}\text{Rb}$  ( $^6\text{Li}$ ) atoms are  $h \times 2.0$  kHz ( $h \times 29.2$  kHz) and  $689.9 a_B^3$  ( $270.8 a_B^3$ ) where  $a_B$  is the Bohr radius and  $h$  is the Planck constant [31, 41]. Tuning the field intensity, we should be able to create a deep optical lattice for Rb atoms to have small enough  $t_b$  comparing to  $t_f$  to reach phases (I)-(IV). Changing the laser frequency can further enhance this capability

to reverse the relative amplitude of interspecies lattice potential [41]. As in experiments only the interspecies s-wave triplet scattering length ( $\sim 20 a_B$ ) between  $^{87}\text{Rb}$  and  $^6\text{Li}$  has been measured [40], the parameters in our model,  $U_{bf}$  and  $J_{bf}$ , cannot be determined. Whether Bose-Fermi density interaction are strong enough to induce DWs requires future experimental developments.

In a harmonic trap potential, three phases (I, V, VI), which have a charge gap in fermions, are expected to occupy a finite spatial range as analogous to formation of Mott insulator shells observed in lattice Bose gases. For other phases which do not have a charge gap, they could be in principle sensitive to trap effects. To detect various magnetic ordering for bosons, we can use the spin-resolved optical Bragg scattering technique [42]. The chiral bosonic magnetic ordering can be identified from triple- $\mathbf{Q}$  peaks in spin structure functions. Its phase boundary can be easily probed in time-of-flight measurements because it is the unique state showing non-zero momentum condensation.

*Conclusion.* We have studied the ground state of a mixture of spin-1 bosons and spin-1/2 fermions in a triangular optical lattice. This spinor Bose-Fermi mixture is found to support interesting magnetic orders, such as non-coplanar, coplanar, and collinear spin orders. Most significantly, relatively weak Bose-Fermi interaction and bosonic tunneling lead to a triple- $\mathbf{Q}$  chiral magnetic order, featuring spontaneous quantum Hall effect in fermions and finite-momentum condensation in bosons. Quantum and thermal fluctuation effects on top of the static spin textures could give rise to dynamical gauge fields [43–45], which is open for future study.

*Acknowledgement.* X.L. would like to thank helpful discussions with A. Rahmani. This work is supported by AFOSR (FA9550-12-1-0079), ARO (W911NF-11-1-0230), DARPA OLE Program through ARO and The Pittsburgh Foundation and the Charles E. Kaufman Foundation (Z.X., W. V. L.). X.L. acknowledges support by JQI-NSF-PFC and ARO-Atomtronics-MURI. Work at Innsbruck is supported by the SFB FOQUS of the Austrian Science Fund, and ERC Synergy Grant UQUAM.

- 
- [1] J. Dalibard, F. Gerbier, G. Juzeliūnas, and P. Öhberg, *Rev. Mod. Phys.* **83**, 1523 (2011).
- [2] N. R. Cooper, *Advances in Physics*, **57**, 539 (2008).
- [3] M. Aidelsburger, M. Atala, S. Nascimbue, S. Trotzky, Y.-A. Chen, and I. Bloch, *Phys. Rev. Lett.* **107**, 255301 (2011).
- [4] K. Jiménez-García, L. J. LeBlanc, R. A. Williams, M. C. Beeler, A. R. Perry, and I. B. Spielman, *Phys. Rev. Lett.* **108**, 225303 (2012).
- [5] M. Aidelsburger, M. Atala, M. Lohse, J. T. Barreiro, B. Paredes, and I. Bloch, *Phys. Rev. Lett.* **111**, 185301 (2013).
- [6] H. Miyake, G. A. Siviloglou, C. J. Kennedy, W. C. Burton, and W. Ketterle, *Phys. Rev. Lett.* **111**, 185302 (2013).
- [7] Y.-J. Lin, K. Jimnez-Garca, and I. B. Spielman, *Nature (London)* **471**, 83 (2011).
- [8] J.-Y. Zhang et al., *Phys. Rev. Lett.* **109**, 115301 (2012).
- [9] P. Wang, Z.-Q. Yu, Z. Fu, J. Miao, L. Huang, S. Chai, H. Zhai, and J. Zhang, *Phys. Rev. Lett.* **109**, 095301 (2012).
- [10] L. W. Cheuk, A. T. Sommer, Z. Hadzibabic, T. Yefsah, W. S. Bakr, and M. W. Zwierlein, *Phys. Rev. Lett.* **109**, 095302 (2012).
- [11] J. Struck, C. Ölschläger, R. Le Targat, P. Soltan-Panahi, A. Eckardt, M. Lewenstein, P. Windpassinger, and K. Sengstock, *Science* **333**, 996 (2011).
- [12] J. Struck, C. Ölschläger, M. Weinberg, P. Hauke, J. Simonet, A. Eckardt, M. Lewenstein, K. Sengstock, and P. Windpassinger, *Phys. Rev. Lett.* **108**, 225304 (2012).
- [13] P. Hauke, O. Tieleman, A. Celi, C. Ölschläger, J. Simonet, J. Struck, M. Weinberg, P. Windpassinger, K. Sengstock, M. Lewenstein, and A. Eckardt, *Phys. Rev. Lett.* **109**, 145301 (2012).
- [14] C. V. Parker, L. C. Ha, and C. Chin, *Nature Physics* **9**, 769 (2013).
- [15] K. Ohgushi, S. Murakami, and N. Nagaosa, *Phys. Rev. B* **62**, R6065 (2000).
- [16] Y. Taguchi, Y. Oohara, H. Yoshizawa, N. Nagaosa, and Y. Tokura, *Science* **291**, 2573 (2001).
- [17] R. Shindou and N. Nagaosa, *Phys. Rev. Lett.* **87** 116801 (2001).
- [18] I. Martin and C. D. Batista, *Phys. Rev. Lett.* **101**, 156402 (2008).
- [19] Y. Akagi and Y. Motome, *J. Phys. Soc. Jpn.* **79**, 083711 (2010).
- [20] Y. Akagi, M. Udagawa, and Y. Motome, *Phys. Rev. Lett.* **108**, 096401 (2012).
- [21] J.-y. Choi, S. Kang, S. W. Seo, W. J. Kwon, and Y.-i. Shin, *Phys. Rev. Lett.* **111**, 245301 (2013).
- [22] M. W. Ray, E. Ruokokoski, S. Kandel, M. Möttönen, and D. S. Hall, *Nature (London)* **505**, 657 (2014).
- [23] A. Griesmaier, Jörg Werner, S. Hensler, J. Stuhler, and T. Pfau, *Phys. Rev. Lett.* **94**, 160401 (2005).
- [24] M. Vengalattore, S. R. Leslie, J. Guzman, and D. M. Stamper-Kurn, *Phys. Rev. Lett.* **100**, 170403 (2008).
- [25] B. Pasquiou, E. Maréchal, G. Bismut, P. Pedri, L. Vernac, O. Gorceix, and B. Laburthe-Tolra, *Phys. Rev. Lett.* **106**, 255303 (2011).
- [26] M. Lu, N. Q. Burdick, and B. L. Lev, *Phys. Rev. Lett.* **108**, 215301 (2012).
- [27] K. Aikawa, A. Frisch, M. Mark, S. Baier, A. Rietzler, R. Grimm, and F. Ferlaino, *Phys. Rev. Lett.* **108**, 210401 (2012).
- [28] Y. Eto, H. Saito, and T. Hirano, *Phys. Rev. Lett.* **112**, 185301 (2014).
- [29] Y. Kawaguchi, H. Saito, and M. Ueda, *Phys. Rev. Lett.* **97**, 130404 (2006).
- [30] S. Yi and H. Pu, *Phys. Rev. Lett.* **97**, 020401 (2006).
- [31] S. De and I. B. Spielman, *Appl. Phys. B* **114**, 527 (2014).
- [32] D. M. Stamper-Kurn and M. Ueda, *Rev. Mod. Phys.* **85**, 1191 (2013).
- [33] Y. Kawaguchi and M. Ueda, *Physics Reports* **520**, 253 (2012).
- [34] T.-L. Ho, *Phys. Rev. Lett.* **81**, 742 (1998).

- [35] T. Ohmi and K. Machida, *J. Phys. Soc. Jpn.* **67**, 1822 (1998).
- [36] M. Houbiers, H. T. C. Stoof, W. I. McAlexander, and R. G. Hulet, *Phys. Rev. A* **57**, R1497 (1998).
- [37] K. M. O'Hara, M. E. Gehm, S. R. Granade, S. Bali, and J. E. Thomas, *Phys. Rev. Lett.* **85**, 2092 (2000).
- [38] P. P. Orth, D. L. Bergman, and K. L. Hur, *Phys. Rev. A* **80**, 023624 (2009).
- [39] G.-W. Chern and C. D. Batista, *Phys. Rev. Lett.* **109**, 156801 (2012).
- [40] C. Silber, S. Günther, C. Marzok, B. Deh, Ph.W. Courteille, and C. Zimmermann, *Phys. Rev. Lett.* **95**, 170408 (2005).
- [41] M. S. Safronova, B. Arora, and C. W. Clark, *Phys. Rev. A* **73**, 022505 (2006).
- [42] T. A. Corcovilos, S. K. Baur, J. M. Hitchcock, E. J. Mueller, and R. G. Hulet, *Phys. Rev. A* **81**, 013415 (2010).
- [43] D. Banerjee, M. Dalmonte, M. Müller, E. Rico, P. Stebler, U.-J. Wiese, and P. Zoller, *Phys. Rev. Lett.* **109**, 175302 (2012).
- [44] E. Zohar, J. Ignacio Cirac, and B. Reznik, *Phys. Rev. Lett.* **109**, 125302 (2012).
- [45] L. Tagliacozzo, A. Celi, A. Zamora, and M. Lewenstein, *Annals of Physics* **330**, 160 (2013).